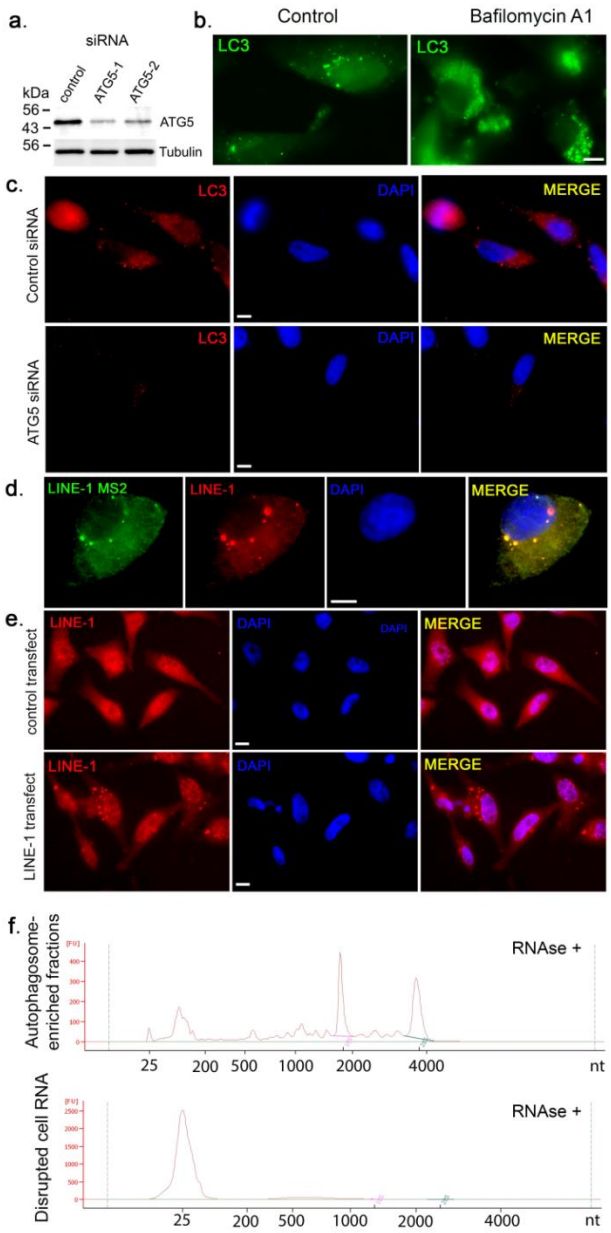

Supplementary Figure 1. Reagents used to detect LC3 and LINE-1 are specific. (**a**) Western blot analysis of ATG5 and TUBA (loading control) cells treated with control siRNA or siRNA targeting ATG5. (**b**) Immunofluorescent detection of LC3 in cells treated with vehicle or Bafilomycin A1 (20 h, 400 nM). (**c**) Immunofluorescent detection of LC3 in cells treated with control siRNA or siRNA targeting ATG5. (**d**) Fluorescent microscopy of cells labeled with FISH probes recognizing LINE-1 (red) and transfected with LINE-1-MS2 and MS2-GFP. (**e**) Fluorescent microscopy of cells labeled with FISH probes recognizing LINE-1 in cells transfected with control plasmid (pcDNA3.1) or plasmid expressing LINE-1 (99 RPS-GFP PUR). All scale bars are 10 µM. (**f**) Agilent Bioanalyzer analysis of RNA from disrupted total cells or from autophagosome-enriched fractions pre-treated with RNAse A and T1. Experiments were performed in triplicate.

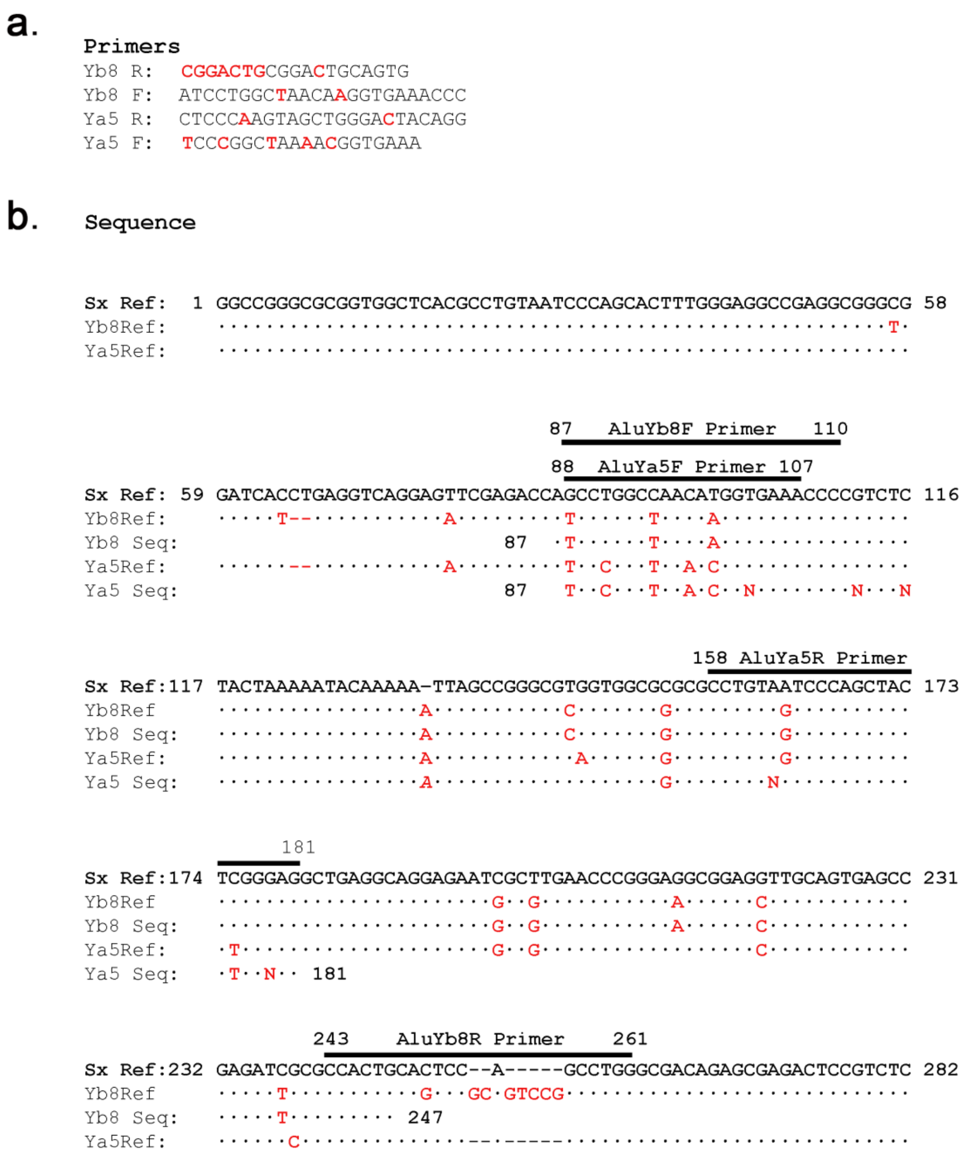

Supplementary Figure 2. Specificity of RT-qPCR analysis for *AluYb8* and *AluYa5* elements. (**a**) Primers used for RT-qPCR analysis of *AluYb8* and *AluYa5* elements. Nucleotides that differentiate *AluYb8* and *AluYa5* are highlighted in red. (**b**) Sequence alignment of reference sequences for *Alu* elements of the *Sx* (Sx Ref)*, Ya5* (Ya5 Ref)*,* and *Yb8* (Yb8 Ref) families*.* Products of RT-qPCR reactions with primers for *AluYa5* and *AluYb8* were sequenced to ensure the targeted RNAs were amplified (Yb8 Seq, Ya5 Seq). Conserved nucleotides are noted with a (-), while non-conserved nucleotides are highlighted in red, unidentified nucleotides from sequencing reactions are indicated by N. The position of the primers on reference sequences are indicated by bold lines. Sequenced *AluYb8* products match exactly the reference sequence for *AluYb8*. Sequenced *AluYa5* products match several diagnostic nucleotides that differentiate *AluYa5* from *AluYb8* and *AluSx*, but several nucleotides could not be confidently identified. These may be due to problems with SAP treatment of Sybrgreen qPCR products or polymorphisms among the 2640 copies of *AluYa5* in the genome.

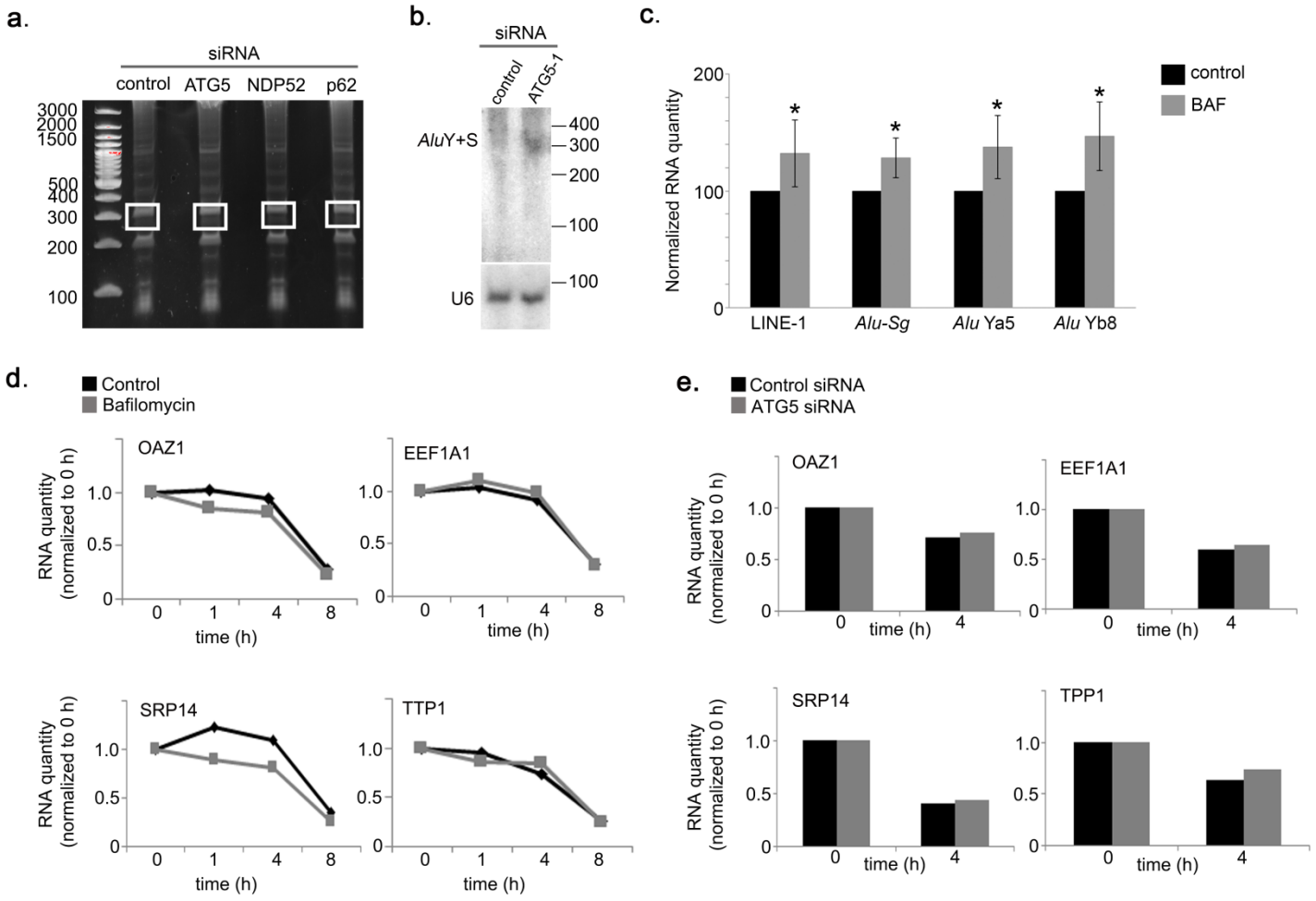

Supplementary Figure 3. Inhibiting autophagy causes levels of retrotransposons to accumulate. Reagents used to detect ORF1p, NDP52 and p62 are specific. (**a**) Representative gel used to extract 250-350 nucleotide RNA for RT-qPCR analysis of *Alu* RNA. Regions extracted are highlighted by white boxes. (**b**) Northern blot analysis of RNA from cells treated with siRNA targeting ATG5 or control, with probes recognizing *AluYa5* and *AluYb8*. U6 RNA serves as a loading control. (**c**) RT-qPCR analysis of the abundance of LINE-1 (5'UTR) and *AluYa5* and *AluYb8* in cells treated with vehicle or Bafilomycin A1 (20 h, 400 nM, n=3, p=0.044 LINE-1, p=0.014 *Alu*Sg, p=0.045 *Alu*Ya5, p=0.013 *Alu*Yb8, ANOVA). (**d**) RT-qPCR analysis of additional control RNAs in cells treated with DMSO or Bafilomycin (400 nM) and actinomycin D. (5nM). (**e**) RT-qPCR analysis of additional control RNAs in pulse-labeled RNA recovered 0 h and 4 h after pulse in cells transfected with siRNA targeting ATG5 or control (10 nM). All experiments were performed in three times.

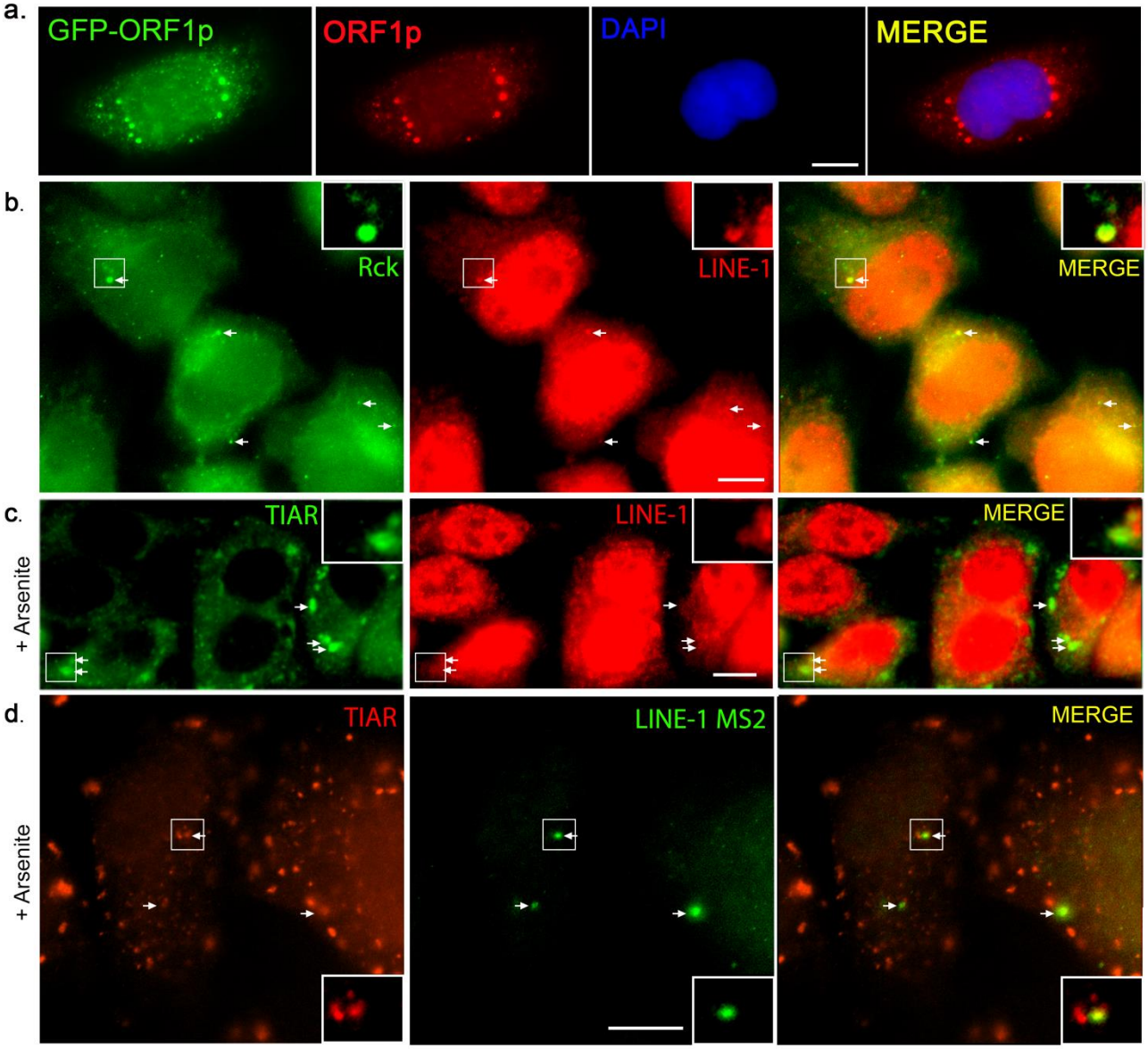

Supplementary Figure 4. LINE-1 RNA localizes with P-bodies and stress granules. (**a**) Fluorescent microscopy of cells transfected with GFP-ORF1p and labeled with anti-ORF1p antibody. (**b**) Fluorescent microscopy of Rck and LINE-1 (FISH). (**c**) Fluorescent microscopy of TIAR (stress granules) and LINE-1 (FISH) in cells treated with arsenite (1 h, 0.5 mM). (**d**) Fluorescent microscopy of TIAR in cells transfected with LINE-1-MS2 and MS2-GFP and treated with arsenite (1 h, 0.5 mM). All scale bars are 10 µM. Experiments were performed a minimum of twice.

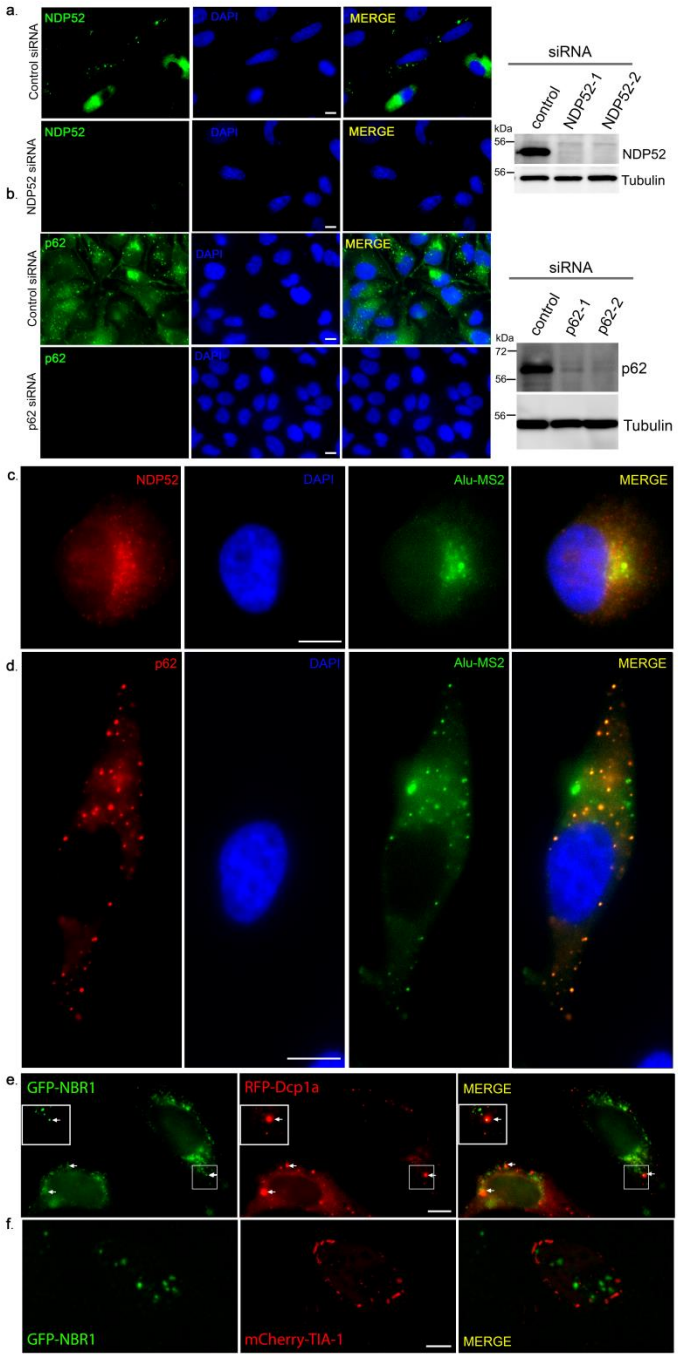

Supplementary Figure 5. *Alu* RNA co-localizes with NDP52 and P62, NBR1 co-localizes with some P-bodies. (**a,b**) Western blot and immunofluorescent microscopy analysis of P62 and NDP52 in cells treated with control siRNA or siRNA targeting NDP52 (**a**) or P62 (**b**). (**c,d**) Fluorescent microscopy of NDP52 (**c**) or P62 (**d**) in cells transfected with *Alu*-MS2 and MS2-GFP. (**e**,**f**) Fluorescent microscopy of cells transfected with GFP-NBR1 and (**e**) RFP-DCP1A or (**f**) mCherry-TIA-1. GFP-NBR1 co-localizes with a subset of RFP-DCP1A foci (P-bodies), but no co-localization with foci of mCherry-TIA-1 (stress granules) was observed. All scale bars are 10 µM. Experiments were replicated at minimum two times.

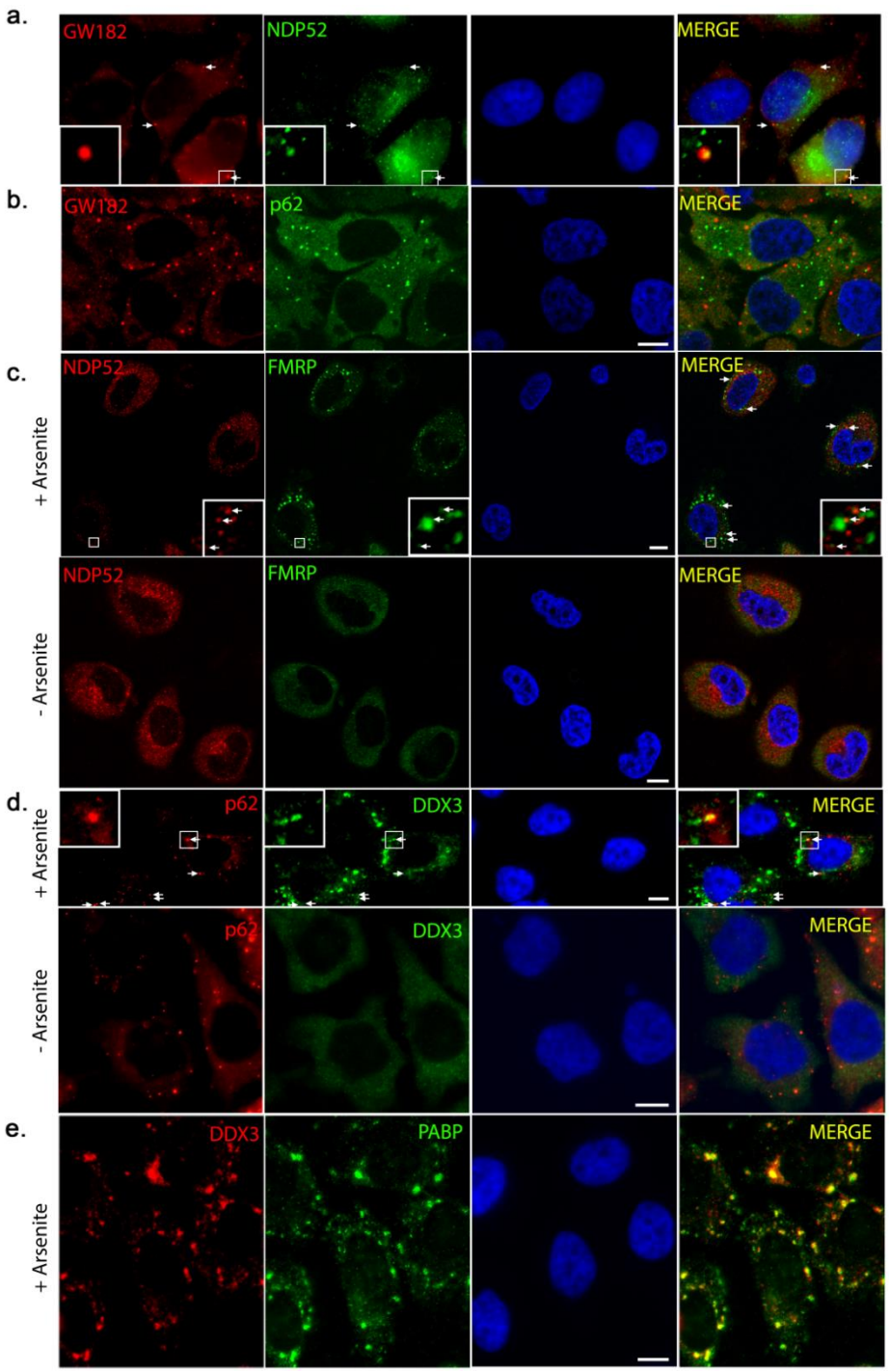

Supplementary Figure 6. NDP52 and P62 co-localize with endogenous markers of P-bodies and stress granules respectively. NDP52 (**a**) but not p62 (**b**) co-localizes with a subset of P-bodies labeled with serum recognizing GW182. (**c**) NDP52 does not co-localize with a marker of arsenite-induced stress granules (FMRP) [1] in the absence or presence of arsenite (1 h, 0.5 mM). (**d**) p62 co-localizes with a subset of arsenite-induced stress granules (1 h, 0.5 mM) labeled with DDX3[2]. (**e**) DDX3 co-localizes with a marker of stress granules (PABP) in cells treated with arsenite. All scale bars are 10 µM. Experiments were performed a minimum of two times each.

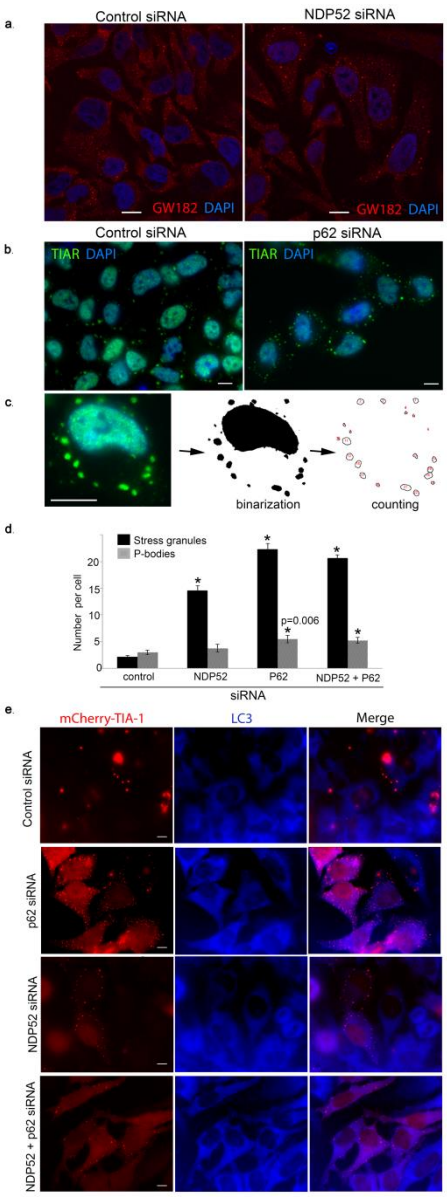

Supplementary Figure 7. Depletion of P62 and NDP52 causes stress granules and P-bodies to accumulate. (**a**) Representative images of P-bodies (serum 18033 recognizing GW182) in cells treated with siRNA targeting NDP52 or control. (**b**) Representative images of stress granules (TIAR) in cells treated with siRNA targeting p62 or control. (**c**) Example of the process used to quantify stress granules and P-bodies. Thresholds were set according to methods and images were binarized to black and white. Punctae from 0.5 to 10 pixel area were automatically counted using the Particle Analyzer function of ImageJ. (**d**) Relative number of foci of GFP-DCP1A or mCherry-TIA-1 in cells treated with siRNA targeting NDP52, P62, both or control. N=98 cells, 1638 stress granules, 466 P-bodies. (n=3, NDP52 $p=7x10^{-9}$stress granules; p62 $p=1x10^{-10}$ stress granules, p=0.006 P-bodies; NDP52+p62 p=3 x 10^{-13} stress granules, p=0.005 P-bodies). (**e**) Representative images of stress granules in cells treated with siRNA targeting p62, NDP52, both NDP52 and p62, or control. All scale bars are 10 µM.

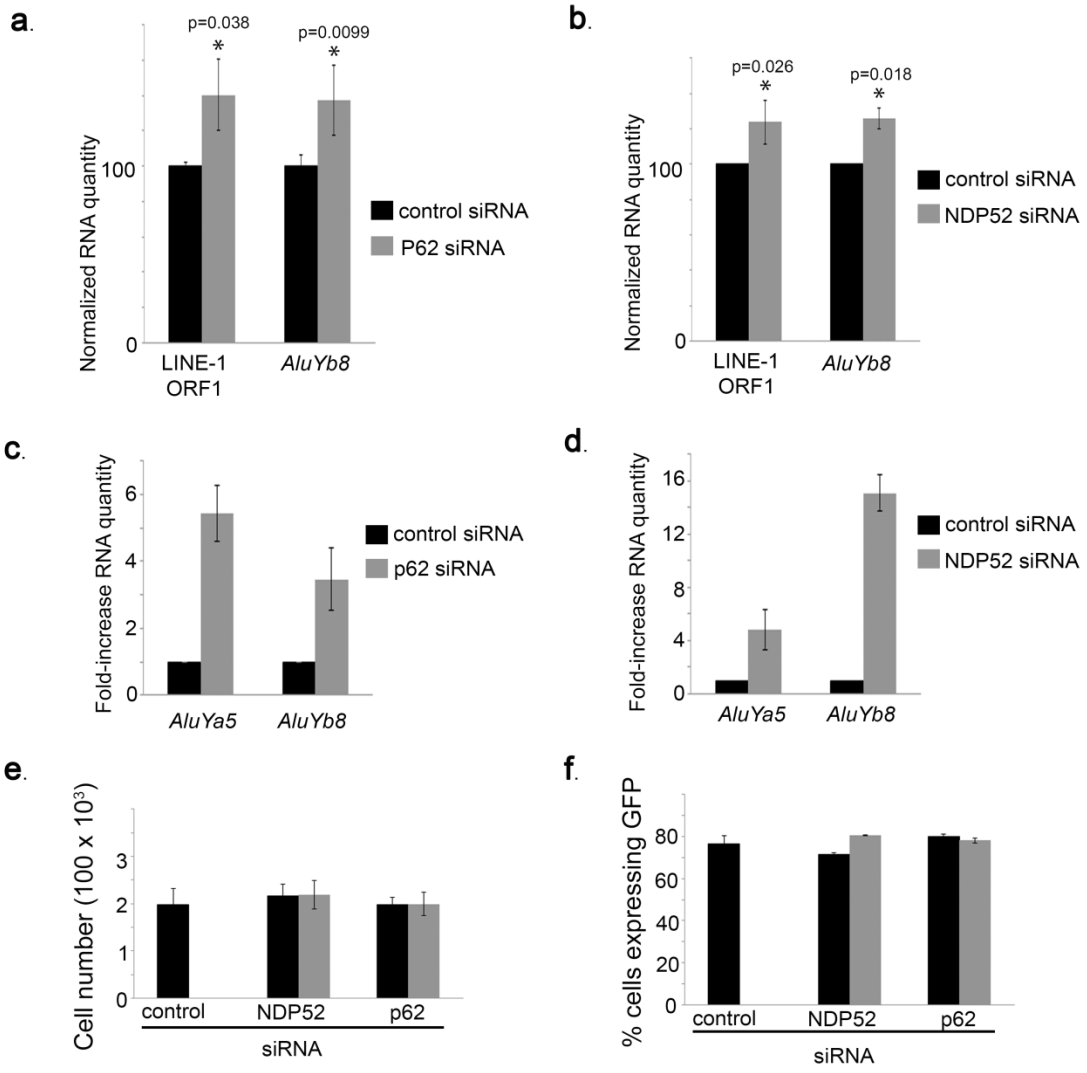

Supplementary Figure 8. Depletion of P62 and NDP52 causes retrotransposon RNA to accumulate. (**a**,**b**) RT-qPCR analysis of levels of LINE-1 RNA (ORF1) and *AluYb8* in cells transfected with siRNA targeting (**a**) P62, (**b**) NDP52 or control. (**c,d**) RT-qPCR analysis of levels of *AluYa5* and *AluYb8* among RNA of 250-350 nt in cells transfected with siRNA targeting p62 (**c**) or NDP52 (**d**). (**e**) Percent of cells expressing GFP when co-transfected with plasmid expressing GFP and either of two independent siRNA (black and grey bars) targeting NDP52, P62 or control (n=3). (**f**) Relative number of cells at experiment's termination if cells were transfected with either of two independent siRNA targeting NDP52, P62 or control (black and grey bars).

Supplementary References

1 Mazroui, R. *et al.* Trapping of messenger RNA by Fragile X Mental Retardation protein into cytoplasmic granules induces translation repression. *Hum Mol Genet* **11**: 3007-3017, (2002).

2 Shih, J. W. *et al.* Critical roles of RNA helicase DDX3 and its interactions with eIF4E/PABP1 in stress granule assembly and stress response. *Biochem J* **441**: 119-129, (2012).